An Electronically Stabilized Phased Array System for Shipborne Atmospheric Wind Profiling

D. C. LAW, S. A. MCLAUGHLIN, M. J. POST, B. L. WEBER, D. C. WELSH, AND D. E. WOLFE

NOAA/Environmental Technology Laboratory, Boulder, Colorado

D. A. MERRITT

Science and Technology Corporation, Boulder, Colorado

(Manuscript received 25 June 2001, in final form 16 October 2001)

ABSTRACT

The design, construction, and first results are presented of a 915-MHz Doppler wind profiler that may be mounted on a moving platform such as a mobile land vehicle, ocean buoy, or a ship. The long dwell times in multiple beam directions, required for the detection of weak atmospheric radar echoes, are obtained by a passive phased array antenna, controlled by a motion control and monitoring (MCM) computer that acquires platform motion measurements and compensates in real time for the platform rotations. The platform translational velocities are accounted for in the signal processing system (SPS) before the calculation of the wind velocity profiles. The phased array antenna, MCM, and SPS are described, and radar-derived wind profiles are compared with those from rawinsonde balloons released during the first test cruise of the system, as the NOAA R/V *Ronald H. Brown* performed ship maneuvers.

1. Introduction

The meteorologic research community has identified the need for wind measurements over the oceans for such applications as studies of the marine boundary layer (Fairall et al. 1997), improved severe weather forecast of coastal areas (Ralph et al. 1999), and studies of El Niño–Southern Oscillation (ENSO) events (Webster and Lukas 1992). The adaptation of ground-based radar wind profilers (RWPs) for shipboard applications has proven to be a formidable engineering challenge. Limited deck space, the harsh marine environment, high levels of radar sea clutter, and the need for antenna stabilization to achieve the beam-pointing accuracy over long dwell times all indicate the need for a system specifically designed for shipborne or buoy-mounted wind profiling (Post et al. 1996).

The National Oceanic and Atmospheric Administration (NOAA) Environmental Technology Laboratory (ETL) has developed such a system. Figure 1 shows the location of the 915-MHz phased array antenna on the NOAA Research Vessel (R/V) *Ronald H. Brown.* The 2.75-m-diameter by 1-m-tall antenna is mounted rigidly to the ship. The 10° (half-power beamwidth) RWP beam is sequentially switched among five beam directions (one vertical beam and four beams, 15° from zenith, in the north, east, south, and west directions), and radar return signals are averaged for about 30 s. A sealed fiberglass radome encloses the phased array antenna, radio frequency (RF) power amplifier and preamplifier, power supplies, and heating/cooling units. The computers and other radar electronics are located in a climate-controlled space in the interior of the ship.

The system incorporates three main improvements over previous NOAA designs used for shipboard wind profiling (Carter et al. 1992; Fairall et al. 1997): three-angle electronic versus two-angle mechanical stabilization; lower antenna sidelobes at low elevation angles for improved sea clutter rejection without the use of large metallic clutter-reducing panels (Russell and Jordan 1991); and advanced signal-processing techniques incorporating 5-beam processing, multiple spectral peak picking, and time–height consistency. Figure 2 shows a diagram of the electronically stabilized RWP system. The radar computer, operating as it does for fixed land-based wind profiling, selects the earth-relative beam direction and communicates its choice to the motion control and monitoring (MCM) computer. The MCM then steers the phased array antenna beam to the earth-relative direction while compensating in real time for the ship orientation, as measured by a commercial GPS-based inertial attitude, position, and velocity measuring system. The antenna beam position is updated at up to

Corresponding author address: Daniel C. Law, NOAA R/ET2, 325 Broadway, Boulder, CO 80305.
E-mail: daniel.c.law@noaa.gov

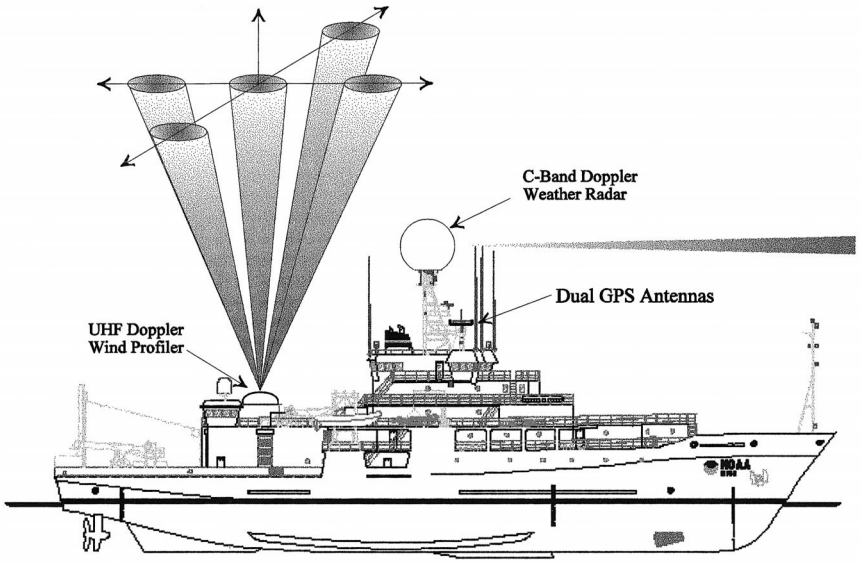

FIG. 1. Mounting location of 915-MHz profiler antenna on NOAA R/V *Ronald H. Brown.* Beam directions are typically 0° and 15° off-zenith in four azimuthal directions, in contrast to the conventional horizontally scanning C-band Doppler weather radar.

10 Hz to accommodate maximum ship roll rates. The signal-processing computer processes Doppler velocity spectra produced by the radar computer into radial wind velocities while combining ship velocities from the MCM to generate meteorologic products and also archives all radar and ship motion data. The user computer is used to display meteorologic products.

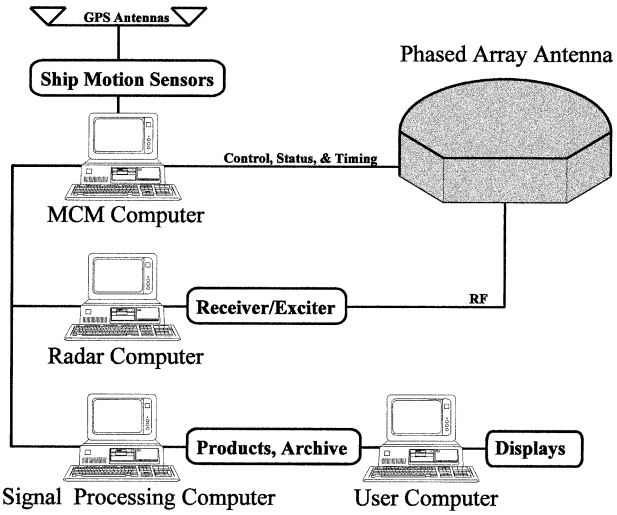

FIG. 2. Electronically stabilized profiler system consists of the phased array antenna and four computers. The MCM computer steers the antenna beam to compensate for ship motion indicated by GPS-based inertial attitude, position, and velocity measurements. The radar computer controls the timing and signal processing to Doppler spectrum. The signal-processing computer detects and identifies atmospheric signals, performs translational motion compensation, and generates meteorologic products. Products are displayed by the user computer.

2. Motion compensation

There are two parts to motion compensation with a shipborne Doppler radar: compensation for rotational motion (i.e., pitch, roll, and heading of the ship) and compensation for translational motion (i.e., course speed, transverse, and vertical movements). Without compensation, ship rotations and translations alter the radar antenna beam pointing direction, and introduce Doppler shifts in the velocity measurements. Both motions contribute to wind measurement errors.

For the ETL shipborne RWP, rotational motion compensation is performed using an electronically steered phased array antenna (section 3), and translational motion compensation is performed in signal processing (section 5). The RWP uses the Doppler beam swinging (DBS) technique, for which meteorological winds are derived from radial velocity measurements collected from several different radar antenna beam pointing directions. Ground-based radars use a number of antenna beams (typically three or five), with orientations fixed relative to the earth. One antenna beam is directed vertically to observe vertical motion, and the other (obliquely directed) beams are tilted slightly off-vertical, typically 15°, and distributed in azimuth in order to observe other components of wind.

The phased array RWP antenna is fixed securely to the ship without any mechanical stabilization to compensate for ship rotational motion. The five earth-relative antenna beam pointing directions are maintained by electronically steering the antenna beam to compensate for the rotational motion of the ship. The antenna beam may be steered to more than 30° off boresight (the di-

rection normal to the flat plane of the antenna), and over 360° in azimuth with an angular resolution of 0.5°.

One of the five predetermined antenna beam pointing directions is set for each radar dwell time on the order of 30 s, the period necessary to generate one smoothed radar Doppler spectrum. Many radar pulses are transmitted, usually at an interval of tens of microseconds, during this dwell period. Radar returns from the atmosphere are observed for each transmitted pulse, with typically hundreds of consecutive observations coherently averaged in order to increase signal-to-noise ratio (SNR). Then, consecutive time series of these coherently averaged observations are used to derive several spectral estimates, which are incoherently averaged in order to increase detectability of weak radar return from the atmosphere (Strauch et al. 1984).

The roll, pitch, and heading angles, and u, v, and w velocity components of the antenna location on the ship are provided by the motion measuring system at a data rate of 100 Hz and acquired by the MCM computer. While rotational and translational motion during one pulse period (tens of microseconds) may be negligible, motion over the 30-s radar dwell period may be significant.

To compensate for angular motion, antenna beam steering is performed by adjusting the phases of 90 individual radar antenna elements. The phases are set to achieve antenna-relative beam pointing angles (θ_A, ϕ_A), where θ_A is the angle off antenna boresight, and ϕ_A is the azimuth angle counterclockwise from the bow of the ship. These angles are computed at 10 Hz in order to maintain antenna beam pointing angles relative to the earth (θ_E, ϕ_E), where θ_E is the angle from vertical, and ϕ_E is the angle clockwise from true north, using the formula

$$\begin{pmatrix} \sin\theta_A \cos\phi_A \\ \sin\theta_A \sin\phi_A \\ \cos\theta_A \end{pmatrix} = \begin{pmatrix} 1 & 0 & 0 \\ 0 & \cos\alpha & \sin\alpha \\ 0 & -\sin\alpha & \cos\alpha \end{pmatrix} \begin{pmatrix} \cos\beta & 0 & \sin\beta \\ 0 & 1 & 0 \\ -\sin\beta & 0 & \cos\beta \end{pmatrix} \begin{pmatrix} \cos\gamma & -\sin\gamma & 0 \\ \sin\gamma & \cos\gamma & 0 \\ 0 & 0 & 1 \end{pmatrix} \begin{pmatrix} \sin\theta_E \cos\phi_E \\ -\sin\theta_E \sin\phi_E \\ \cos\theta_E \end{pmatrix}, \quad (1)$$

where α is the ship roll angle (positive with downward roll of starboard), β is the ship pitch angle (positive with bow pitch upward), and γ is the ship heading (positive clockwise from true north).

If V_{RS} is a radial velocity measurement, including the effects of ship motion, then the estimate of radial velocity relative to the earth, V_{RE}, is

$$V_{RE} = V_{RS} - V_S, \quad (2)$$

where V_S is the Doppler shift introduced by the ship motion:

$$V_S = S_S \cos(\theta_E) \cos(\phi_E - \phi_S) - W_S \sin(\theta_E), \quad (3)$$

where S_S is the speed, ϕ_S is the course, and W_S is the vertical velocity of the antenna on the ship. The ship motion data are relative to the position of the antenna on the ship. This is important because ship rotations cause translational velocity at the antenna that is a function of its location on the ship. To compensate for translational motion, the velocity components acquired from the ship motion sensors are averaged for the duration of the radar dwell time and used in (2) to calculate the earth-relative Doppler velocities for the stabilized beam directions above. Note that ship motion with periods less than the dwell time still broaden the Doppler spectra, but the motion compensation removes the mean ship velocity from the radial velocity estimates.

3. Electronically stabilized phased array antenna

Figure 3 shows the positions of the 90 identical elements in the phased array antenna. To simplify the RF feed network, there is no center element. The elements are arranged in an equilateral triangular lattice with 0.66-wavelength spacing (21.6 cm at 915 MHz). This spacing allows grating lobe-free steering at any azimuth for off-boresight (θ_0) angles up to 35°. This is large enough to accommodate platform pitch-and-roll angles up to 20° with antenna beams that are 15° from zenith. Maximum steering angles of 25° are anticipated, based on ship motion records from the *Ronald H. Brown* under typical sea conditions. Figure 4 shows a block diagram of the phased array antenna. The implementation is a *passive* phased array, one that does not incorporate amplification in the transmit or receive paths of each element (Mailloux 1994). This architecture is typically simpler and less expensive than an *active* phased array but also has performance limitations, which will be discussed. The 500-W (peak) pulsed RF transmit signal is split and distributed to each of the 90 antenna element modules (AEMs). To electronically steer the radar beam, the MCM commands a microcontroller in each AEM to shift the signal phase. Received RF signals are likewise phase-shifted and combined. Timing signals ensure that phase switching is synchronized to the radar pulse repetition period (section 4).

The triangular spacing and the hexagonal outline of the array results in antenna radiation patterns with sidelobes that are more circularly symmetric and generally lower than the square arrays, with elements arranged in a square lattice commonly used for 915-MHz boundary layer RWPs (Ecklund et al. 1988). Since sea clutter is much stronger for vertically polarized radiation, partic-

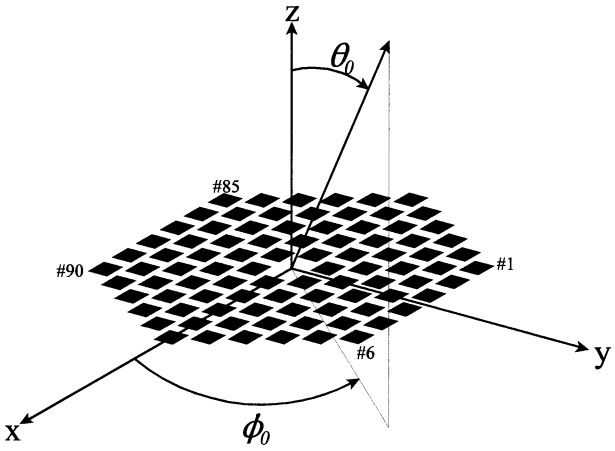

FIG. 3. Antenna elements (90) are arranged in a hexagonal aperture with equilateral triangular spacing of 0.66-λ. There is no element at the center of the array. The phase of the RF signal at each element is adjusted to steer the beam to the coordinates (θ_0, ϕ_0).

ular care was taken in the antenna design to minimize it (section 4). Figure 5a shows the computed antenna gain pattern for the array steered 20° off-zenith, assuming uniform amplitude distribution on the 90 elements. To further reduce the low-elevation sidelobes responsible for ground and sea clutter, conventional aperture amplitude distributions, such as Taylor, Dolph–Chebyshev, and $\cos^x$ on a pedestal distributions (Hansen 1998), were considered. These distributions either sacrifice too much antenna gain or needlessly reduce sidelobes in noncritical directions. Instead, a Fourier transform technique (Mailloux 1994) was employed to custom design the amplitude distribution for this application. This technique allows the designer to trade off sidelobe suppression for decreased gain or increased sidelobes in noncritical directions. In the final design, the low-elevation sidelobes were selectively reduced only over the anticipated range of antenna steering directions ($0° \leq \theta_0 \leq 25°$, for all ϕ_0).

Figure 6 shows the amplitude distribution on the 90-element hexagonal array of Fig. 3 as a function of the element distance from the center of the array. Maximum power is applied to the elements in a ring halfway between the center and outer edge of the array. The six elements at apexes of the outer edge of the hexagon have the minimum power; one-tenth or −10 dB, relative to the maximum power. Figure 5b shows the resulting computed antenna gain pattern for the array steered 20° off-zenith as in Fig. 5a. Figure 7 compares cuts through the principal plane (one that contains the main beam and significant sidelobes) for the two distributions. Compared to the uniform distribution, the annular distribution reduces low-elevation sidelobes by 7–10 dB, over the most likely steering angles. Note, however, that the first sidelobes nearest to the main beam are higher and wider for the annular distribution, and it also costs 0.5 dB in main beam gain. An attempt to steer the beam by more than about 25° off boresight (not shown) results in horizontal sidelobes slightly higher than the array with uniform distribution.

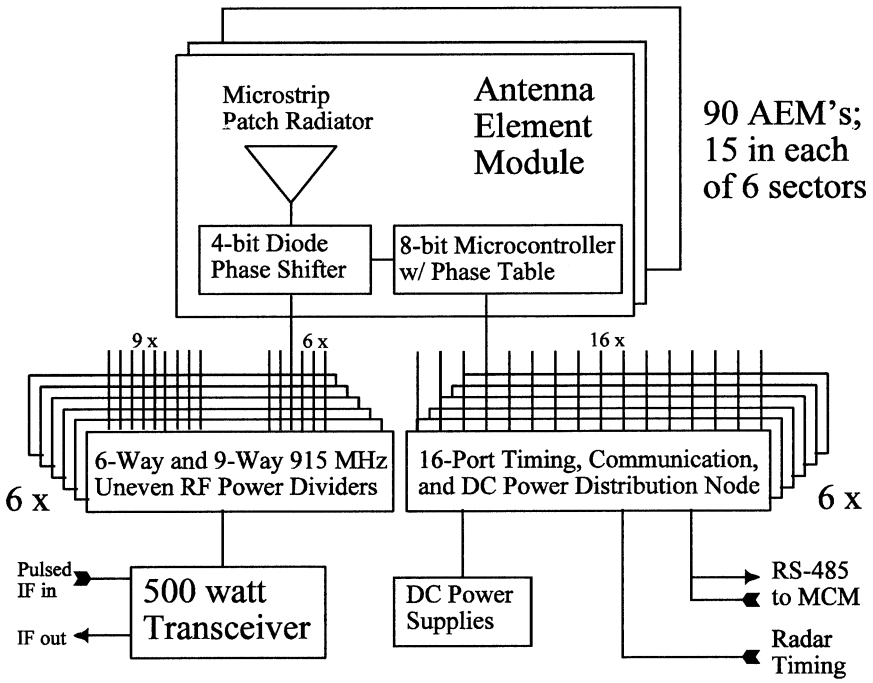

FIG. 4. Block diagram of the shipborne wind profiler radar antenna assembly. Identical AEMs (90) interface to RF and digital distribution networks. These components are enclosed in a fiberglass radome and rigidly mounted to the ship.

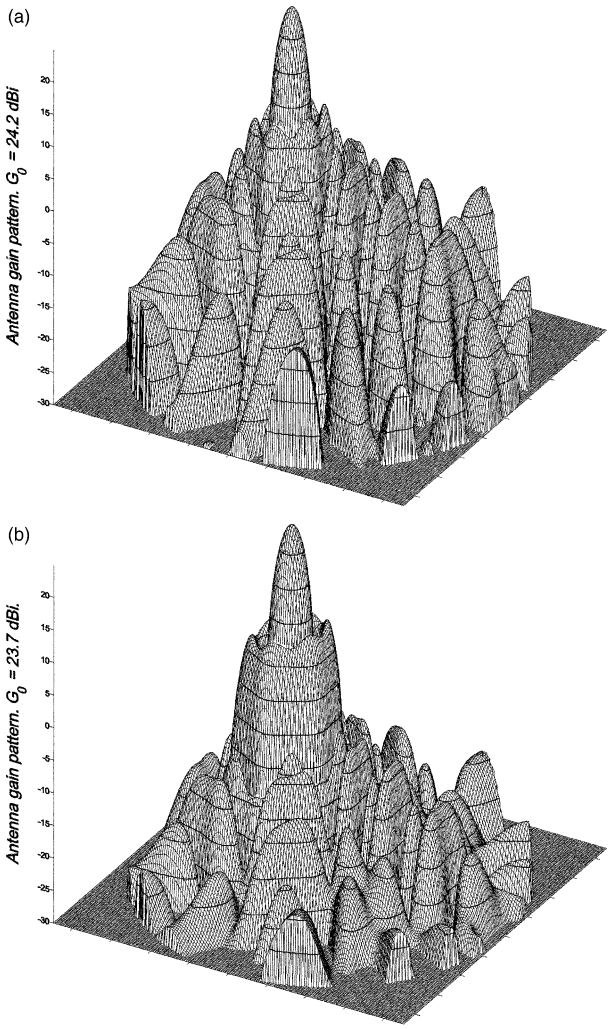

FIG. 5. (a) Computed antenna radiation pattern of a beam steered to $(\theta_0, \phi_0) = (20°, 90°)$ in Fig. 3, for a uniform aperture amplitude distribution. Zenith angle is plotted as the radius from the center of the plot (the circular periphery corresponds to $\theta = 90°$). (b) Computed radiation pattern for a beam steered as in (a), but using the annular aperture distribution of Fig. 6. Horizontal sidelobes are −40 dB (w.r.t. beam peak). In practice, −35 dB is achievable.

Computed horizontal sidelobe levels for this steering direction are −40 dB relative to the main beam gain of 23.7 dBi. Using a calibrated antenna test range, −35 dB horizontal sidelobes were measured. The 5-dB deficit is probably due to amplitude and phase errors at the elements and to the effects of the finite array size not accounted for in the computer model. Based on measurements of other antenna arrays used for land and shipboard profiling, the new phased array represents an improvement of 10–15 dB (one way) over previous designs. However, the total RF losses through the power dividers, distribution cables, and phase shifters is 2.5 dB, about 1.5 dB higher than conventional land-based RWPs.

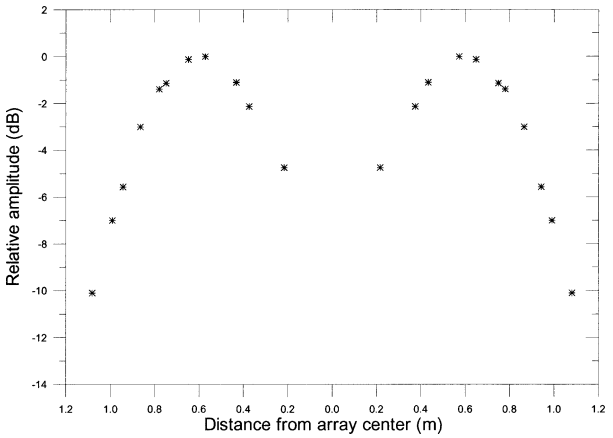

FIG. 6. Relative amplitude on the elements as a function of distance from the center of the array. Highest RF power is applied to an annulus at one-half the array radius. The six apex elements have one-tenth the power. There is no element at the center of the array.

4. Antenna element module

The AEMs shown in Fig. 4 are 215 mm × 185 mm × 75 mm (8.5″ × 7.3″ × 3.0″) replaceable units weighing 2.5 kg (5.5 lbs). Each sealed aluminum module contains an 8-bit microcontroller, a switched-line phase shifter, and a microstrip patch antenna, arranged in a *tile* architecture (Mailloux 1994), and costs $750 to manufacture.

The MCM (bus master) communicates with all of the AEMs (slaves) over a 4-wire multidrop RS-485 serial network using a commercial communication protocol. An address (1–90), unique to its position in the array (Fig. 3), is programmed into the microcontroller in each AEM when it is installed in the array. The MCM may address and issue commands to an individual AEM, or it may issue commands to address 0, which are executed

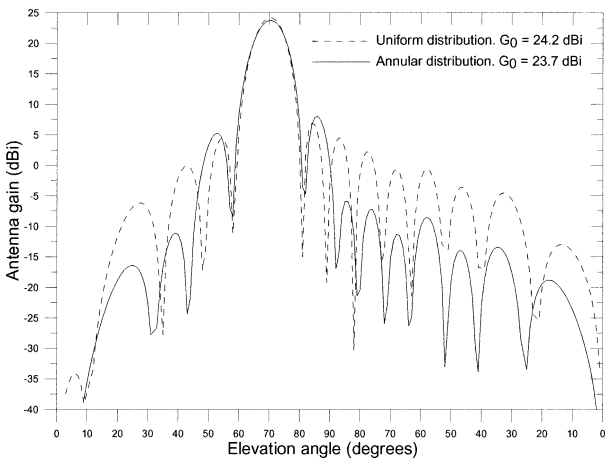

FIG. 7. Principal-plane cuts through the antenna patterns of Fig. 5. Annular aperture amplitude distribution improves antenna sidelobes by about 10 dB over most steering angles. Reduction of these sidelobes comes at the cost of 0.5 dB reduced gain, and higher and wider first sidelobes near the main beam.

simultaneously by all AEMs. Additional radar timing signals are distributed to all modules using RS-422/485 balanced differential drivers and receivers. The microcontroller board includes a 128-kbyte nonvolatile memory, which is programmed by the MCM with the phase lookup table (LUT) unique to each module's position (and address) in the array.

For a desired antenna-relative beam pointing direction (θ_0, ϕ_0) in Fig. 3, the required phase for an element at location (x_0, y_0) is

$$\psi = -\frac{2\pi}{\lambda}[x_0 \sin(\theta_0) \cos(\phi_0) + y_0 \sin(\theta_0) \sin(\phi_0)], \quad (4)$$

where λ is the wavelength. The small bandwidth requirement (<1%) of the RWP allows the use of ψ mod (2π), which limits the largest required phase shift to less than one wavelength. Computer simulations verify that a 4-bit phase shifter (with 22.5° phase resolution) is required to limit the beam pointing error to 1° over all steering angles. The phase LUT in each AEM relieves the MCM of the task of computing and communicating the required phase for each of the modules. Instead, it broadcasts the required antenna-relative beam direction, and the AEMs adjust their phases independently and simultaneously in synchronization with the radar timing signals. The microcontroller also has an 8-channel, 8-bit A/D converter, which is used to measure module temperature, voltage, and RF power levels. The MCM polls all of the modules sequentially and maintains a status map of the array that is updated about every 60 s.

In order to meet mechanical and electrical requirements, the 4-bit diode phase shifter was custom designed using an RF computer-aided design (CAD) system for simulating the operation of the RF switching diodes and optimizing the resulting impedance match, transmission loss, and insertion phase of the shifter. The shifter has an insertion loss of 0.9 dB and an rms phase and amplitude error over all phase angles of less than 1° and 0.1 dB, respectively. The circuit also includes a dual-directional coupler that allows the measurement of forward and reflected RF power. This is used to monitor the antenna and phase shifter circuitry because a failure in these components results in high reflected power.

To provide sufficient bandwidth and to minimize the low-elevation radiation (particularly for vertical polarization), the rectangular microstrip patch antenna is printed on the underside of a 0.79-mm-thick fiberglass board and positioned in an air-filled cavity 6.35 mm (0.25″) above the aluminium ground plane. The feed point impedance is adjusted to 55-j25 Ω to compensate for mutual coupling among elements. The antenna array return loss is greater than 22 dB over all azimuth angles and zenith angles up to 35°, and the array exhibits no scan blindness.

5. Signal processing

Radar wind profiling makes use of the Doppler beam swinging technique to produce vertical profiles of the horizontal and vertical wind averaged over a desired sample time. The radar determines the wind speed by measuring the Doppler shift of the return signals scattered from turbulent fluctuations of refractive index as a function of range from several (three to five) antenna beam positions (Balsley and Gage 1980; Strauch et al. 1984; Rottger and Larsen 1990; Ecklund et al. 1990). One antenna beam is pointed toward zenith and the other beams are pointed off zenith (usually 10°–20°). Velocity measurements from all the beams are combined to produce a profile of winds. The 5-beam pointing sequence used on the shipborne profiler is repeated every 2.5 min. In this RWP technique, a time series of phase-coherent radar returns from the atmosphere is sampled over many transmitted radar pulses and used to generate spectra, from which Doppler shifts may be measured.

In a stationary (land based) 3-beam system, the radial velocity derived from the vertical antenna beam is used to remove the vertical component from the velocity measurements made on the oblique beams. With the 5-beam system it is possible to remove the effects of vertical motion and also to estimate meteorological variations by examining data from the different antenna beams. Radar return on different antenna beams in the Doppler beam swinging technique observes different volumes of the atmosphere, which may be separated by a few kilometers at higher altitudes. The wind velocity may vary over these separations caused by turbulence, wave motion, and other atmospheric motions. With observations from a moving ship, the volume of atmosphere observed on any given antenna beam during a dwell period (~30 s) changes slightly as the ship translates horizontally.

Operation of the radar and signal processing up to the generation of smoothed radar Doppler spectra are performed using the Profiler On-line Program (POP), which was developed by NOAA's Aeronomy Laboratory and is available commercially. Time–domain integration and spectral processing of time series effectively remove out-of-band contaminating signals and noise, improving signal-to-noise ratio for radar return from the atmosphere. Spectral smoothing improves detectability of weak signals in the presence of noise. The signal processing discussed in detail here begins with these smoothed Doppler radar spectra.

The ETL signal processing consists of four separate processing modules: (i) calculation of the noise floor and the detection of all signals in each radar Doppler spectrum; (ii) the estimation of spectral moments (i.e., power, radial velocity, and spectral width) for all signals detected; (iii) the identification of signals to be associated with radar return from the atmosphere; and (iv) the generation of meteorological products. All of these signal-processing steps are tied together by and rely

upon a system-independent, portable database engine specifically targeted for RWPs.

The ETL signal-processing system (SPS) differs substantially from the traditional system, in which processing is linear and sequential throughout and where only one signal per Doppler spectrum is ever detected and reported. Fundamental to this signal processing is the realization that, even with attempts to suppress possible contamination from ground and sea clutter, radio frequency interference (RFI), spurious signals, noise, etc., RWP-averaged Doppler spectra may contain multiple signals. The SPS removes the constraint of being restricted to a single data channel while addressing the possibility of multiple signals in a single spectra. Multiple data channels (at different ranges, at different times, and on different antenna beams) have been effectively employed for years (Weber and Wuertz 1991) in postprocessing and quality control of meteorological products. The ETL SPS employs algorithms that require multiple data channels to reliably detect atmospheric signals.

The SPS includes four processing modules: Signal Detection (SigDetect), Multiple Moments Estimation (MultiMom), Signal Identification (SigID), and Meteorological Products Estimation (MetProd). Each of these four modules runs as a separate process and contain a number of signal processing algorithms.

Data flow is linear and sequential in SigDetect and MultiMom. In these two modules, each RWP-averaged Doppler spectrum is processed independently and only once. On the other hand, data flow in SigID, and to a lesser degree in MetProd, is necessarily recursive and elaborate. In order to identify RWP return from the atmosphere (SigID) and derive meteorological products (MetProd), it is necessary to consider signals and their associated measurements at different ranges, at different times, and in different antenna beams.

a. Signal detection module (SigDetect)

Signal detection is accomplished in a two-step process. First, the system noise threshold is determined using a statistical model (Hildebrand and Sekhon 1974). Second, spectral values above the noise threshold are separated into different signal domains for later identification. SigDetect addresses the possibility of overlapping signals. The recognition of multiple signals in the presence of noise is accomplished by detecting maxima above the noise threshold based on a defined minimum detection level (1.25σ above the mean noise floor). Each maxima is searched to the right and left until either the noise floor or a local minimum is encountered. Uncertainty in the spectral estimates, calculated as part of the statistical model, is used in assigning significance to the maxima and local minima. Overlapping signals are identified as part of this process.

b. Multiple moments module (MultiMom)

Spectral moments (power, Doppler velocity, and spectral width) are estimated using a centroid method for all peaks identified in SigDetect. The combined set of spectral moments is used to assist in the identification of each signal with its physical source. An uncertainty is also computed as part of the estimates of the spectral moments and used later in calculating a confidence factor. No attempt is made at this point to separate out the true atmospheric signal, but only to pass on all potential signals with additional statistical information. The Doppler velocity for each of the signals identified by SigDetect is corrected for ship translational motion (section 2).

c. Signal identification module (SigID)

Traditionally, signal identification was based upon the assumption of simple spectra, containing only white system noise and one atmospheric signal per spectrum per data channel. This assumption may be violated when the atmospheric signal is weak or in the presence of strong ground or sea clutter, point targets, and/or RFI.

Consistency over time and over space (height and antenna beams) is the most general principle affecting confidence in signal identification. Consistency is usually applied to Doppler velocity, but it may be also applied to the other spectral moments. Note that consistency does not always mean continuity. For example, the velocity may appear to be discontinuous in time at transitions between clear air and precipitation, and in height across a melting layer or elevated frontal zone, depending upon the sampling.

Signals from the atmosphere may be classified by their physical characteristics. In general, these signals fall into two categories: precipitation and clear air (winds). Some excellent classifications and descriptions can be found in Ralph (1995), Ralph et al. (1996) and Wuertz et al. (1988). Precipitation signatures are related to the types of precipitation (snow, rain, hail, etc.), which are known to have different fall velocities. The broadening effect precipitation has on the spectra and the fact that many different types of precipitation exist simultaneously can hide or overlap weaker clear air signals.

It should be noted that signal classifications are not exact. Using the information described above to classify signals, the SigID process selects which of the multiple moment estimates calculated by MultiMom best describes an atmospheric signal. The identification is based on four characteristics: (i) magnitude of the signals, (ii) persistence of signal over range, (iii) persistence of signal over time, and (iv) persistence of signal across antenna beams. Each of these characteristics is calculated for each of the first three spectral moments: power, velocity, and spectral width. Therefore, there are 12 (4 characteristics times 3 spectral moments) char-

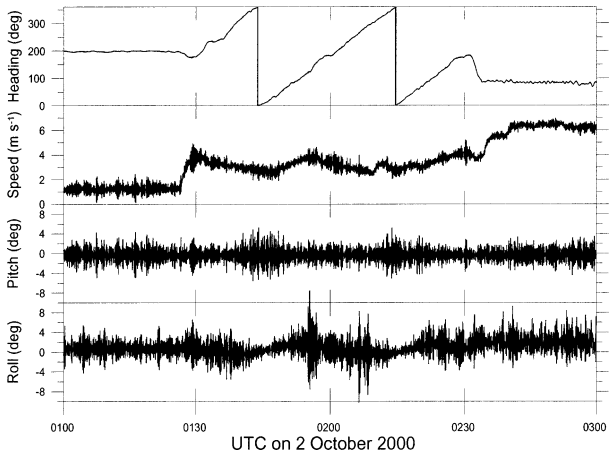

FIG. 8. Ship motion from 0100 to 0300 UTC 2 October 2000. Wind profiler operated in full compensation mode as the ship made two complete circles at a speed of ~4 m s^{-1}. A rawinsonde balloon was launched from the ship at 0216 UTC.

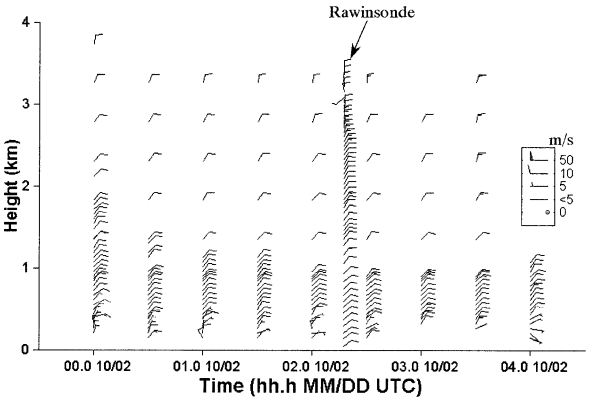

FIG. 9. Half-hour-averaged wind profiles (60- and 500-m resolution) before, during, and after the circular ship maneuver from 0100 to 0300 UTC 2 October 2000. Rawinsonde-derived wind profile is shown at 0216 UTC.

acteristic measurements calculated for each signal identified. These 12 characteristics are used to select the atmospheric signals that are further processed by a time–height continuity process (Weber and Wuertz 1991; Weber et al. 1993).

For each signal identified in a spectrum a confidence factor is calculated. This confidence factor is based on the uncertainty in estimates of the first three spectral moments, signal-to-noise ratio, signal-to-clutter ratio (clutter is the total power in all signals), range continuity, time continuity, and cross-beam continuity. The moments, calculated from one signal in each beam that has the most consistency in terms of its characteristics, are retained as the signal for processing into wind data. These same moments can also be used for calculation of turbulence quantities.

d. Meteorological products module (MetProd)

For each beam MetProd calculates an estimate of radial wind velocity and its uncertainty, from atmospheric moments identified in SigID using a least squares fit over a user-defined time grid (30 min). These same data can next be gridded in height if desired. For the results presented in this paper, the data were left at their sampled vertical resolution (60 m). After temporal and spatial gridding these radial velocities are combined to produce the standard RWP product, wind speed, and direction profile.

Each calculated wind speed and direction carries with it a joint confidence factor. The individual confidence factors (described above) of atmospheric signals used to produce this wind are multiplied and normalized 0–1 (0 is no confidence, 1 is full confidence) to produce this joint confidence factor. Experience is required to choose a threshold value for joint confidence, above which data may be considered good. This threshold can be site, type of RWP, weather, and application dependent.

6. Field test results

Several experiments were conducted over the period 26 September–7 October 2000 to test the operation of the electronically stabilized wind profiler system aboard the NOAA R/V *Ronald H. Brown* as it sailed from Dutch Harbor, Alaska, to San Diego, California. These included operating the profiler in various configurations, tracking the RF radiation from the sun, collecting time series and spectral data, maneuvering the ship in various ways, and launching rawinsondes for comparisons.

The following experiment was designed to test the *full compensation* mode of the system, wherein the geocentric beam directions are maintained while compensating for ship pitch, roll, and heading changes, and signal processing compensates for ship translational velocities. The 100-Hz ship motion data (relative to the position of the antenna on the ship) were averaged and recorded at 10 Hz. Figure 8 shows the ship heading, speed, pitch, and roll for 0100–0300 UTC 2 October 2000. The ship completed two circles at about 4 m s^{-1} over a 1-h period. Pitch and roll angles were as large as 5° and 10°, respectively, with angular rates (not shown) as high as 4° s^{-1} during the maneuver. The winds were forecast to be relatively constant in speed and direction. A rawinsonde was launched at 0216 UTC, midway through the maneuver. Figure 9 shows half-hour-averaged winds from the profiler for the period 0000–0400 UTC, combined with the rawinsonde wind profile. The profiler winds are calculated from 60- and 500-m-resolution data, and include winds with confidence factors from 0 to 1 (i.e., no confidence filtering). Winds were consistent from NNE at 8–12 m s^{-1}. The agreement is very good, considering the extreme changes in ship speed and attitude during the maneuver. There are profiler inconsistencies in the lowest few heights that

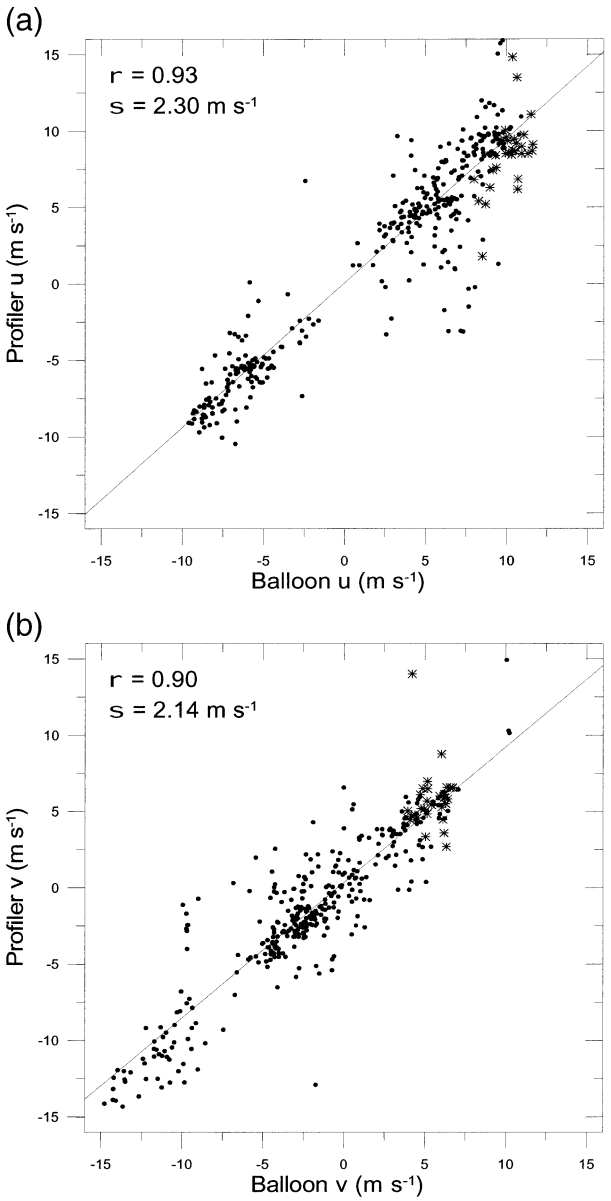

FIG. 10. Comparison of the (a) u component and (b) v component of wind between wind profiler and 15 rawinsonde balloon launches. Stars indicate data collected during the circular ship maneuver test.

may be due to sea clutter, ship clutter, or receiver recovery problems.

Figure 10 shows unedited u- and v-component scatterplots of rawinsonde and profiler wind measurements for 15 balloon flights over a 12-day span as the ship sailed from Dutch Harbor to San Diego. The profiler measurements include both 60-m-resolution, with typical altitudes from 100–1000 m, and 100- and 500-m-resolution data, covering up to 4000-m altitude. The wind profiler times closest to the balloon launch times were selected, and the balloon data were interpolated to match the wind profiler heights. The measurements during the ship circular maneuver test (Figs. 8 and 9) are indicated and show about the same agreement as the other comparisons. The correlation coefficients and rms speed differences of about 0.91 and 2.2 m s^{-1}, respectively, compare favorably to the results of Weber and Wuertz (1990), although their dataset was much larger and the range of wind speed was much greater than in this case.

7. Summary discussion and future work

An improved shipborne radar wind profiler has been constructed and demonstrated. Initial tests show that the system components required for the electronic stabilization and velocity compensation of the phased array wind profiler have been designed and assembled correctly and that the system represents a significant advancement in wind profiler technology for moving platforms. (Further information and photographs are available at http://www6.etl.noaa.gov/projects/ronbrown/.) Preliminary results show agreement with rawinsonde wind measurements comparable to those for fixed land-based UHF profilers. The use of a commercial ship motion measurement system and the reduced sea clutter resulting from the low sidelobe antenna design of the electronically stabilized profiler seem to have reduced two significant problems that have plagued previous shipborne wind profilers (Hartten 1998).

Since the initial test cruise, the wind profiler has been operated on the R/V *Ronald H. Brown* during three other field experiments, along with measurements from the C-band Doppler radar and a Doppler lidar, as well as routine rawinsonde balloon launches. These operations should provide a rich dataset for further comparisons and improvements in profiler design and signal-processing techniques.

The choice of a passive phased array antenna design has performance and operational implications. The need to minimize RF losses required the careful design of low-loss phase shifters requiring about 3 W of power each, and low-loss, uneven power dividers. The additional feed line losses of the passive phased array design resulted in the loss of 30% of the meager (500 W peak, 50 W average) RF transmit power and weak received signals. They also increased the system noise figure, which reduces the system sensitivity. At the expense of higher electric power consumption, a larger RF power amplifier could compensate for these losses. Solid-state heating and cooling units were used to regulate the temperature in the antenna enclosure on the deck. The units are rugged and reliable but inefficient. When operating at maximum capacity, the antenna system consumes about 2.3 kW of electrical power. The rest of the RF and digital electronics consume about 1 kW of power. While these power requirements are appropriate for shipborne installations, they will likely need to be reduced for remote buoy-mounted deployments.

For future systems, active phased arrays, ones that incorporate amplifiers in the transmit and receive paths,

have many advantages. Distributing the RF power amplification among all of the elements increases reliability by eliminating a single point source of failure, and distributes the heat and power supply current densities. The system noise figure may be improved by placing low-noise amplifiers at each element. The ability to dynamically control the amplitude as well as the phase at each element provides additional design flexibility, which would allow the design of optimal antenna radiation patterns with lower sidelobes. Fortunately, inexpensive electronic devices such as low-noise amplifiers, vector modulators, circulators, and power amplifiers, have been developed by the wireless communication industry. The shipborne and buoy-mounted wind profiler systems envisioned over 20 years ago (Balsley and Gage 1980) appear to be economically and technically feasible.

Acknowledgments. NOAA's System Acquisition Office (SAO) and the Office of Global Programs (OGP) sponsored the development of the profiler. Warren Keenan (OGP) and John Hotaling (SAO) provided valuable project and design input. Sergio Pezoa, Tom Ayers, Kevin Knott, and Matt James of ETL assisted in the design, construction, testing, and installation of the system, and B. Boba Stankov of ETL provided Fig. 9. We gratefully acknowledge the assistance of the officers and crew of the NOAA R/V *Ronald H. Brown*, and the helpful suggestions of the anonymous reviewers.

REFERENCES

Balsley, B. B., and K. S. Gage, 1980: The MST radar technique: Potential for middle atmospheric studies. *Pure Appl. Geophys.*, **118,** 452–493.

Carter, D. A., W. L. Ecklund, K. S. Gage, M. Spowart, H. L. Cole, E. F. Chamberlain, W. F. Dabbert, and J. Wilson, 1992: First test of a shipboard wind profiler. *Bull. Amer. Meteor. Soc.*, **73,** 1587–1592.

Ecklund, W. L., D. A. Carter, and B. B. Balsley, 1988: A UHF wind profiler for the boundary layer: Brief description and initial results. *J. Atmos. Oceanic Technol.*, **5,** 432–441.

——, ——, ——, P. E. Currier, J. L. Green, B. L. Weber, and K. S. Gage, 1990: Field tests of a lower tropospheric wind profiler. *Radio Sci.*, **25,** 899–906.

Fairall, C. W., A. B. White, J. B. Edson, and J. E. Hare, 1997: Integrated shipboard measurements of the marine boundary layer. *J. Atmos. Oceanic Technol.*, **14,** 338–359.

Hansen, R. C., 1998: *Phased Array Antennas.* John Wiley and Sons, 486 pp.

Hartten, L. M., 1998: Reconciliation of surface and profiler winds at ISS sites. *J. Atmos. Oceanic Technol.*, **15,** 826–834.

Hildebrand, P. H., and R. S. Sekhon, 1974: Objective determination of the noise level in Doppler spectra. *J. Appl. Meteor.*, **13,** 808–811.

Mailloux, R. J., 1994: *Phased Array Antenna Handbook.* Artech House, 534 pp.

Post, M. J., C. W. Fairall, A. B. White, J. R. Jordan, K. S. Gage, J. Wilson, and L. M. Hartten, 1996: Shipboard wind profiling by radar: Problems and possible solutions. *Proc. 1996 Battlespace Atmospherics Conf.*, San Diego, CA, Naval Command, Control and Ocean Surveillance Center, Tech. Doc. 2938, 567–572.

Ralph, F. M., 1995: Using radar-measured radial vertical velocities to distinguish precipitation scattering from clear-air scattering. *J. Atmos. Oceanic Technol.*, **12,** 257–267.

——, P. J. Neiman, and D. Ruffieux, 1996: Precipitation identification from radar wind-profiler spectral moment data: Vertical velocity histograms, velocity variance, and signal power-vertical velocity correlations. *J. Atmos. Oceanic Technol.*, **13,** 545–559.

——, and Coauthors, 1999: The California Land-Falling Jets Experiment (CALJET): Objectives and design of a coastal atmosphere–ocean observing system deployed during a strong El Niño. Preprints, *Third Symp. on Integrated Observing Systems*, Dallas, TX, Amer. Meteor. Soc., 78–81.

Rottger, J., and M. F. Larsen, 1990: UHF/VHF radar techniques for atmospheric research and wind profiler applications. *Radar in Meteorology: Battan Memorial and 40th Anniversary Radar Meteorology Conference*, D. Atlas, Ed., Amer. Meteor. Soc., 235–281.

Russell, C. A., and J. R. Jordan, 1991: Portable clutter fence for UHF wind profiler radar. Preprints, *Seventh Symp. on Meteorological Observations and Instrumentation*, New Orleans, LA, Amer. Meteor. Soc., J152–J156.

Strauch, R. G., D. A. Merritt, K. P. Moran, K. B. Earnshaw, and D. C. Welsh, 1984: The Colorado wind profiling network. *J. Atmos. Oceanic Technol.*, **1,** 37–49.

Weber, B. L., and D. B. Wuertz, 1990: Comparison of rawinsonde and wind profiler radar measurements. *J. Atmos. Oceanic Technol.*, **7,** 157–174.

——, and ——, 1991: Quality control algorithm for profiler measurements of wind and temperature. NOAA Tech. Memo. ERL WPL-212, 32 pp.

——, ——, and R. McPeek, 1993: Quality control for profiler measurements of winds and RASS temperatures. *J. Atmos. Oceanic Technol.*, **10,** 452–464.

Webster, P. J., and R. Lukas, 1992: TOGA COARE: The Coupled Ocean–Atmosphere Response Experiment. *Bull. Amer. Meteor. Soc.*, **73,** 1377–1417.

Wuertz, D. B., B. L. Weber, R. G. Strauch, A. S. Frisch, C. G. Little, D. A. Merritt, K. P. Moran, and D. C. Welsh, 1988: Effects of precipitation on UHF wind profiler measurements. *J. Atmos. Oceanic Technol.*, **5,** 450–465.